

## SOFT QCD IN ATLAS: MINIMUM-BIAS AND DIFFRACTION STUDIES

*E. K. Sarkisyan-Grinbaum  
for the ATLAS Collaboration*

University of Texas at Arlington, Department of Physics, Arlington, USA  
Department of Physics, CERN, Geneva, Switzerland

We present measurements of charged-particle production in proton–proton collisions at centre-of-mass energies of  $\sqrt{s} = 0.9, 2.36, \text{ and } 7 \text{ TeV}$  recorded with the ATLAS detector at the Large Hadron Collider. Events were collected using a single-arm minimum-bias trigger; charged tracks are measured with high precision in the inner tracking system. Minimum-bias analysis uses data samples at all three energies, while diffractive events are studied using a sample of events at  $\sqrt{s} = 7 \text{ TeV}$ . To study diffractive interactions, the events that have hits on exactly one side of the ATLAS detector were selected. The charged-particle multiplicity, pseudorapidity, and transverse momentum spectra are analyzed and compared to the predictions by various Monte Carlo models.

PACS: 13.75.Cs; 13.85.-t

### INTRODUCTION

The results of soft QCD measurements of charged-particle production in proton–proton collisions at centre-of-mass energies of  $\sqrt{s} = 0.9, 2.36 \text{ and } 7 \text{ TeV}$  using the ATLAS detector [1] at the LHC are presented. The soft, or nonperturbative, QCD processes of multiparticle production include diffractive (single- and double-diffractive) and nondiffractive components forming the inelastic scattering. All these ingredients are not well modeled by perturbative QCD or Monte Carlo (MC) models when applied to low transverse momentum, or soft, particle production [2]. The MC models need to be (re)tuned to the data. An understanding of soft particle production processes is important for precision (high transverse momentum) measurements to be made at the LHC and is crucial for understanding of QCD effects, total cross section determination, understanding of saturation effects, jet studies, mass reconstruction. These measurements should be done early on, at low luminosity, to avoid the effect of overlapping («pile-up») collisions at high luminosities. We present minimum bias [3,4] and diffractive [5] measurements, while another report presents studies of azimuthal spectra and underlying events [6].

The ATLAS detector (A Toroidal LHC ApparatuS) is one of the two large general purpose detectors at the LHC. For the measurements presented here, the trigger system and the tracking devices were of particular importance. The ATLAS Inner Detector (ID) immersed in a 2 T axial magnetic field is used to measure charged particles. It consists of three subdetectors: pixel detector (Pixel), a silicon strip detector (SCT) and a transition radiation tracker. The

inner detector has a full coverage<sup>1</sup> in the azimuthal angle and covers the pseudorapidity range  $|\eta| < 2.5$ .

The ATLAS trigger system is a three-level trigger system. For the measurements presented here, the trigger relies on the Beam Pickup Timing devices (BPTX) and the Minimum Bias Trigger Scintillators (MBTS). The BPTX are composed of electrostatic beam pick-ups attached to the beam pipe at  $\pm 175$  m from the center of the ATLAS detector. The MBTS are mounted at each end of the detector in front of the liquid-argon end-cap calorimeter cryostats at  $z = \pm 3.56$  m and are segmented into eight sectors (16 independent wedge-shaped plastic scintillators) in azimuth and in two rings in pseudorapidity ( $2.09 < |\eta| < 2.82$  and  $2.82 < |\eta| < 3.84$ ). Data were taken for these measurements using the single-arm MBTS trigger, formed of BPTX and MBTS triggers. The MBTS trigger efficiency was studied with a separate prescaled Level-1 BPTX trigger, filtered to obtain inelastic interactions by ID requirements at higher level triggers. The MBTS efficiency was found to be  $> 99\%$ . The two MBTS time measurements were used to veto halo and beam-gas events, as well as a gap trigger for diffractive studies, as described below.

The data at  $\sqrt{s} = 900$  GeV and 2.36 TeV have been recorded in December 2009 and the 7 TeV data, used here, have been recorded in March–April 2010. During the 2.36 TeV data collection, stable conditions were not declared. Therefore, to ensure detector safety, the SCT was in standby mode with lower hit efficiencies and increased noise. To estimate track reconstruction efficiency, two complementary methods were developed [4] to measure the spectra: the first used the full ID information and corrected the efficiency from the simulation using a data-driven technique, while the second used tracks reconstruction from Pixel information only. The results obtained by these methods were found to agree within 3%.

## 1. DATA AND MONTE CARLO

**1.1. Data Selection.** The data used here comprise about 357K selected events at  $\sqrt{s} = 900$  GeV, about  $10^6$  events at  $\sqrt{s} = 7$  TeV, and about 6K events at  $\sqrt{s} = 2.36$  TeV. These data samples correspond to integrated luminosities of approximately 7, 0.1, and  $190 \mu\text{b}^{-1}$  at  $\sqrt{s} = 0.9, 2.36,$  and 7 TeV, respectively.

To reduce the contribution from background events and nonprimary tracks, as well as to minimize the systematic uncertainties, the events were required: to have fired a single-arm Level-1 MBTS trigger, the primary vertex (PV) to be reconstructed using the beam-spot (BS) information, to not have a second primary vertex with four or more tracks in the same bunch crossing (to remove pile-up), and to have at least two good tracks in the event. A good track then is defined as one that satisfies: transverse momentum  $p_T > 100$  MeV ( $> 500$  MeV at  $\sqrt{s} = 2.36$  TeV) and  $|\eta| < 2.5$ ; a hit in the first layer of the Pixel detector; a minimum of one Pixel hit in any of the 3 layers; at least two ( $p_T > 100$  MeV), four

---

<sup>1</sup>The ATLAS reference system is a Cartesian right-handed co-ordinate system, with the nominal collision point at the origin. The anticlockwise beam direction defines the positive  $z$  axis, while the positive  $x$  axis is defined as pointing from the collision point to the centre of the LHC ring and the positive  $y$  axis points upwards. The azimuthal angle  $\phi$  is measured around the beam axis, and the polar angle  $\theta$  is measured with respect to the  $z$  axis. The pseudorapidity is defined as  $\eta = -\ln \tan(\theta/2)$ , and  $p_T$  is the momentum component transverse to the beam direction.

( $p_T > 200$  MeV) or six ( $p_T > 300$  MeV) SCT hits  $N_{\text{sct}}$  at  $\sqrt{s} = 0.9$  and 7 TeV, and  $N_{\text{sct}} > 6$  at  $\sqrt{s} = 2.36$  TeV; the transverse and longitudinal impact parameters relative the PV:  $|d_0| < 1.5$  mm,  $|z_0 \sin(\theta)| < 1.5$  mm, respectively. The residual backgrounds are found to be small or negligible: cosmic ray and beam background  $< 10^{-6}$  and  $< 0.1\%$ , respectively, and pile-up contribution of the order of 0.01%.

Track reconstruction efficiencies were determined from MC (Subsec. 1.2) using full detector simulation and reconstruction. A key issue is the description of material in the tracking volume. This was tuned to match the data. The track reconstruction efficiency is studied as a function of  $\eta$  and  $p_T$ , as shown in Fig. 1 for 0.9 and 7 TeV. The difference in the track reconstruction efficiencies between two energies is dominated by different number and configuration of the disabled Pixel and SCT modules in the running conditions. The trigger, vertex and tracking efficiencies were used to correct the data back to particle level [3,4,7]. Where possible, the data were used to reduce MC dependencies. More details on the determination of efficiencies, backgrounds, uncertainties, and correction procedure can be found in [3,4,7]. It should be noted that no corrections were applied in the diffraction analysis [5].

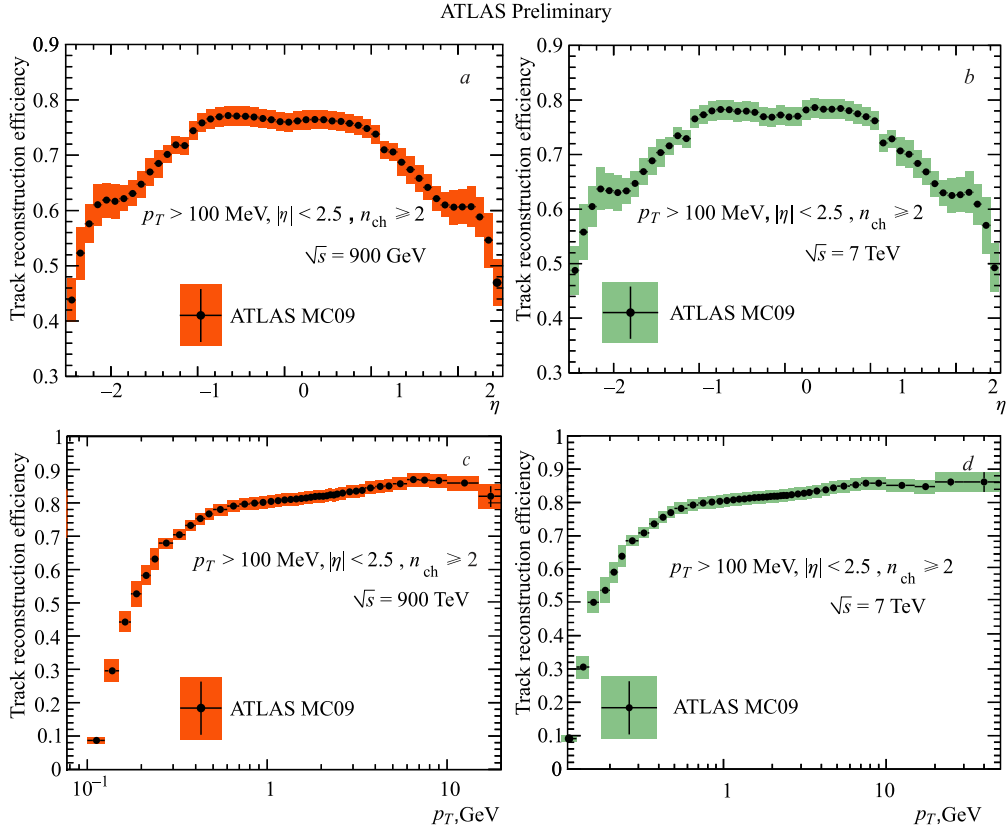


Fig. 1. The track reconstruction efficiency as a function of  $\eta$  (a, b) and  $p_T$  (c, d) as derived from PYTHIA6 tune MC09 (Subsec. 1.1). The statistical errors are shown as black lines, the total errors as shaded areas. The distributions are shown at  $\sqrt{s} = 900$  GeV (left plots) and 7 TeV (right plots)

**1.2. Monte Carlo Models.** The PYTHIA [8] MC generator was used as a main generator in the ATLAS studies. The parameters of this generator have been tuned to describe charged-hadron production and the underlying event in  $pp$  and  $p\bar{p}$  data at energies 0.2 to 1.96 TeV. Samples of single-diffractive, double-diffractive and nondiffractive events were produced using the PYTHIA6 (6.4.21) generator. A specific set of optimized parameters, the ATLAS MC09 PYTHIA6 tune [9], is the reference tune throughout these studies. These parameters were derived by tuning to underlying event and minimum bias data from Tevatron at 0.63 and 1.8 TeV. The MC samples generated with this tune were used to determine detector acceptances and efficiencies and to correct the data. The diffractive and nondiffractive contributions in the generated samples were mixed according to the generator cross sections to describe the inelastic scattering. All the events were processed through the ATLAS detector simulation code [10].

For the purpose of comparing the present measurement to different phenomenological models describing minimum-bias events, the following additional PYTHIA6 samples were generated: the ATLAS data-based AMBT1 tune [11], which was obtained by attempting to fit charged-particle multiplicity distributions in a diffraction limited phase-space; the Perugia0 tune [12], in which soft-QCD part is tuned using only minimum-bias data from the Tevatron and CERN  $p\bar{p}$  colliders; the DW tune [13], which uses the virtuality-ordered showers and was derived to describe the CDF Run II underlying event and Drell–Yan data. In addition, the PYTHIA8 generator [14] was used which includes new features such as hard scattering in diffractive systems, up-to-date parton density function (pdf) set, a possibility of using one pdf set for hard scattering and another for the rest, and finally, the PHOJET generator [15] used as an alternative model where soft processes use Pomeron exchange and semihard processes are described by perturbative parton scattering.

## 2. MINIMUM-BIAS MEASUREMENTS

Figure 2 shows the pseudorapidity distributions measured at  $\sqrt{s} = 0.9$  and 7 TeV. The measurements are by 5 to 20% higher than the MC predictions, except the 900 GeV PHOJET prediction which is on the top of the data. Interestingly, in both the cases, PYTHIA8 is near to the data, being even closer than the AMBT1 model at 7 TeV. At 2.36 TeV, where the distribution is measured at  $p_T > 500$  MeV, the AMBT1 and MC09 tunes slightly underestimate the data, while other MC models are lower by 10–20% than the data.

Figures 3 and 4 show, respectively,  $p_T$  and multiplicity  $n_{\text{ch}}$  distributions of charged particles detected at  $\sqrt{s} = 7$  TeV. The MC  $p_T$  spectra agree well with the data at intermediate  $p_T$  from 0.5 to 2 GeV, while largely disagree at lower and higher  $p_T$ . The data differs from MC predictions at low multiplicities, and at  $n_{\text{ch}} > 40$  PYTHIA tunes underestimate the data by 50%. Similar observations are made from 900 GeV studies and earlier studies at  $p_T > 500$  MeV, as well as from measurements at 2.36 TeV. The deviation is expected due to contribution from diffractive events. Indeed separating the different components of MC models, one finds [3] that the models have very different descriptions of diffraction. PYTHIA6 has no hard diffraction included: the diffraction model used there produces no tracks for  $p_T > 3$  GeV and no diffractive events with  $n_{\text{ch}} > 27$ . PYTHIA8 and PHOJET

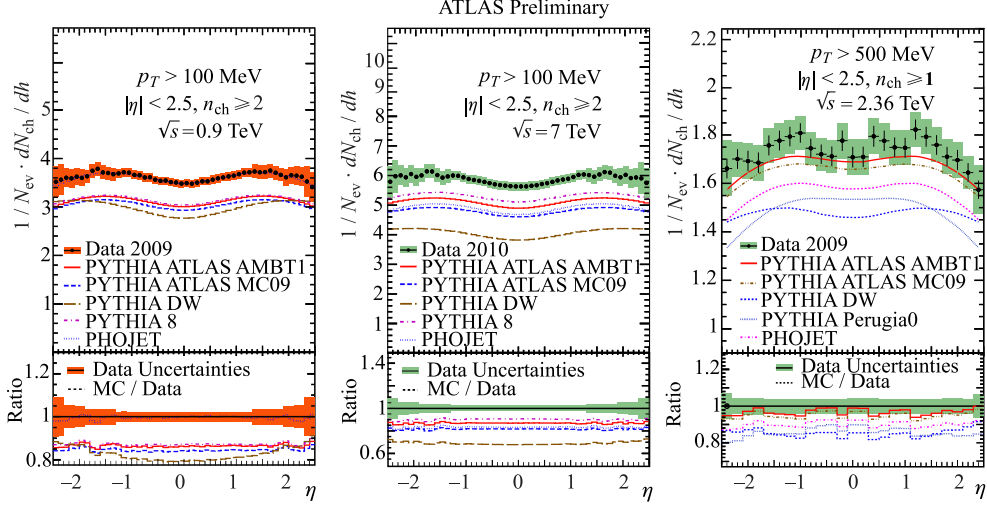


Fig. 2. Charged-particle  $\eta$  spectrum at  $\sqrt{s} = 0.9, 7,$  and  $2.36$  TeV. The distribution at  $2.36$  TeV is for  $p_T > 500$  MeV and with at least one track. The values of the ratio histograms refer to the bin centroids. The data are shown in the same way as in Fig. 1

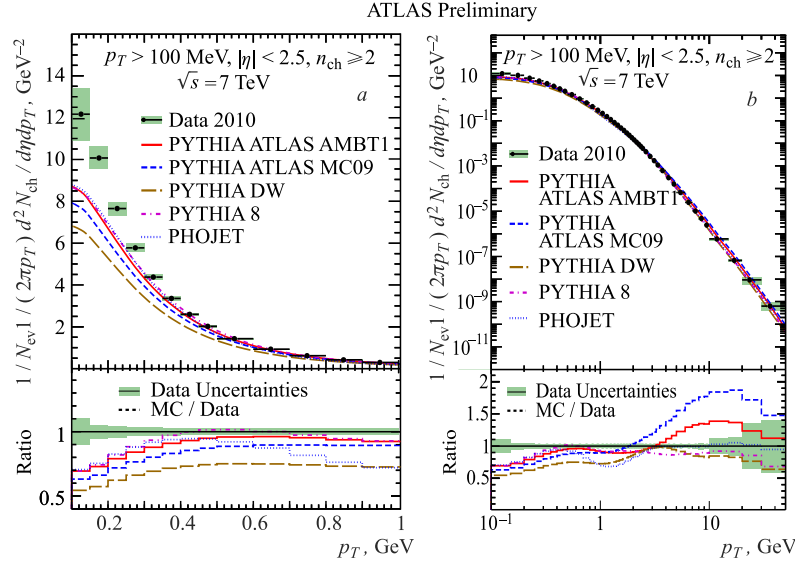


Fig. 3. Charged-particle  $p_T$  spectrum at  $\sqrt{s} = 7$  TeV. Plot *a* shows the distribution in linear scale up to  $p_T = 1$  GeV, and plot *b* shows the full-range distribution in log–log scale. The data are shown in the same way as in Fig. 2

both have a hard component to the diffraction extending up to higher multiplicities. The fraction of diffractive events vs.  $p_T$  is very roughly constant for these two models. All this is more discussed in Sec. 3.

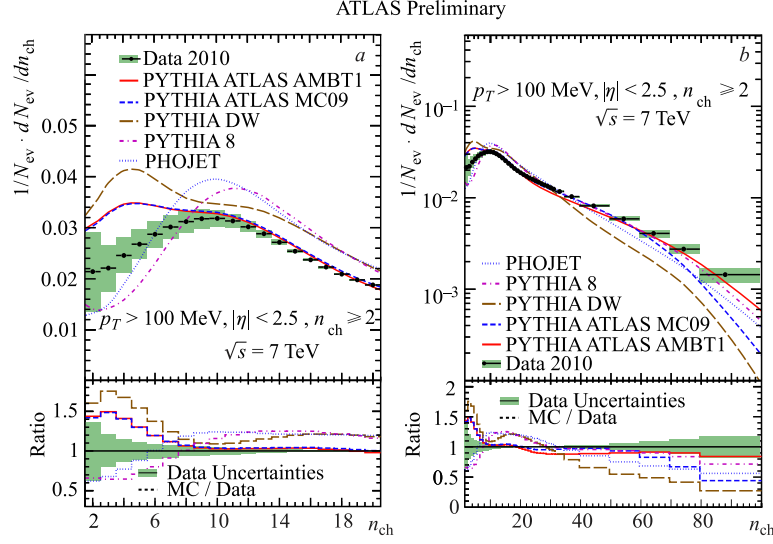


Fig. 4. Charged-particle multiplicities at  $\sqrt{s} = 7$  TeV. Plot *a* shows the distribution in linear scale up to  $n_{\text{ch}} = 20$ , and plot *b* shows the full-range distribution in log scale. The data are shown in the same way as in Fig. 2

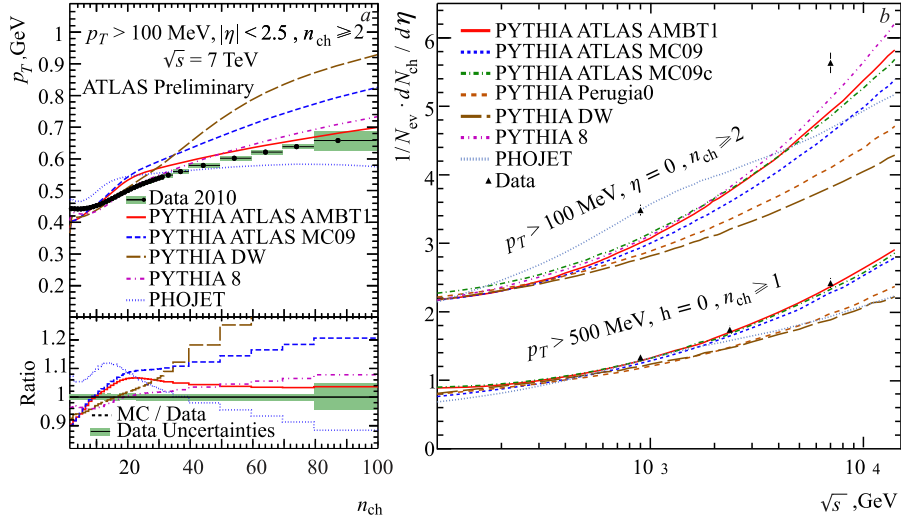


Fig. 5. Plot *a* shows charged-particle averaged  $p_T$  as a function of multiplicity at  $\sqrt{s} = 7$  TeV. The data are shown in the same way as in Fig. 2. Plot *b* shows the central pseudorapidity density as a function of centre-of-mass energy

Figure 5 summarizes the above observations. One can see that no MC model describes the data at low  $n_{\text{ch}}$  and low  $p_T$ , though AMBT1 and PYTHIA8 are close to the data for  $p_T > 500$  MeV. The deviations can be attributed to diffraction.

### 3. DIFFRACTIVE ENHANCED MINIMUM-BIAS STUDIES

Diffraction interactions, generally at low momentum transfer, can only be described by phenomenological models, and there is little consensus in the theoretical community as to which method is the best, leading to high uncertainty in model predictions at LHC energies. This uncertainty results in difficulties for tuning the nondiffractive portion, forcing the MC tunes to be made from phase-space areas where diffractive effects are negligible [9]. Meanwhile, the absence of color exchange in diffractive events leads to rapidity gaps, a characteristic which experimentalists can exploit. Therefore, to enhance the sample in diffraction, events were selected with a hit (in at least one MBTS cell) only on one,  $z$ -positive or  $z$ -negative, side of the MBTS. This requirement preferentially selects single and double-diffractive events. Double-diffractive events pass the selection if the mass of the diffractive system on one of the two sides is small enough that all the particles escape at  $|\eta| > 3.84$  and thus do not create a signal in the MBTS. The study uses the 7 TeV data corresponding to an integrated luminosity of  $\sim 23 \mu\text{b}^{-1}$ . The tracks selection criteria are similar to the above, while requiring  $p_T > 500 \text{ MeV}$ ,  $|d_0^{\text{BS}}| < 1.5 \text{ mm}$ ,  $|z_0| < 100 \text{ mm}$ , and  $N_{\text{sct}} \geq 6$ , where  $z_0$  is defined with respect of the origin of the detector coordinate system. This event selection does not require a primary vertex, to avoid any bias at low track multiplicity. In addition a subset of events (the «single-sided» sample) was selected by vetoing events that have hits on both sides of the MBTS. The main systematic uncertainties were found to arise from beam backgrounds, data and MC agreement for the MBTS simulation and the tracking performance, and were carefully investigated [5].

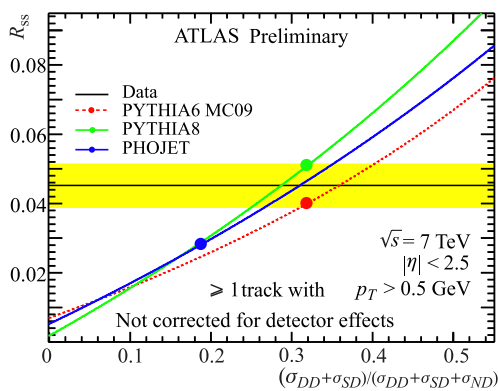


Fig. 6. The ratio  $R_{\text{ss}}$  of events with hits only on one side of the MBTS scintillators to events with any hits in the MBTS scintillators as a function of the diffractive contribution to the total inelastic cross section. The values for the cross sections used by these MC programs and the corresponding values of  $R_{\text{ss}}$  are indicated by the solid circles. The ratio of the single-to-double diffractive cross sections is held fixed to the generator prediction

Figure 6 shows the measured fraction  $R_{\text{ss}}$  of the number of the «single-sided» events to the number of such events that have any hit in either side of the MBTS, compared to the Monte Carlo predictions. The measured value is  $R_{\text{ss}} = (4.52 \pm 0.02(\text{stat.}) \pm 0.61(\text{syst.}))\%$ . The predictions from PYTHIA6 MC09 (4.01%) and PYTHIA8 (5.11%) agree well with the data while the PHOJET prediction (2.83%) falls short by 70% corresponding to  $2.9\sigma$ . The diffractive component needs to be increased from 20 to 30% in PHOJET to describe the data.

To investigate the event kinematics, the  $\eta$ ,  $p_T$ , multiplicity  $n_{\text{track}}$ , and  $\Delta\eta$ <sup>1</sup> distributions were measured. As is seen in [5], the data on  $\eta$  spectrum is flat about 0.4, well modeled by PYTHIA8 and PHOJET, while underestimated by about 30% by PYTHIA6. Study of the  $\Delta\eta$  spectrum shows [5] that at low  $\Delta\eta$  all three generators describe the data well but at high  $\Delta\eta$ , where the diffractive processes dominate, PYTHIA6 underestimates the measurements.

Figures 7 and 8 show charged-particle low-multiplicity and  $p_T$  distributions, respectively. One can see that multiplicity distribution falls by five orders of magnitude over the range of 1 to 20 tracks. It is thus much steeper than that measured in the inclusive sample [3]. It is well modeled both by PYTHIA8 and PHOJET, while the PYTHIA6 predicts smaller multiplicities than the data apart from the tail, where the nondiffractive contribution plays a role. The  $p_T$  spectra predicted by PHOJET are in excellent agreement with the data, while PYTHIA8 predicts slightly softer spectrum, and PYTHIA6 even much softer.

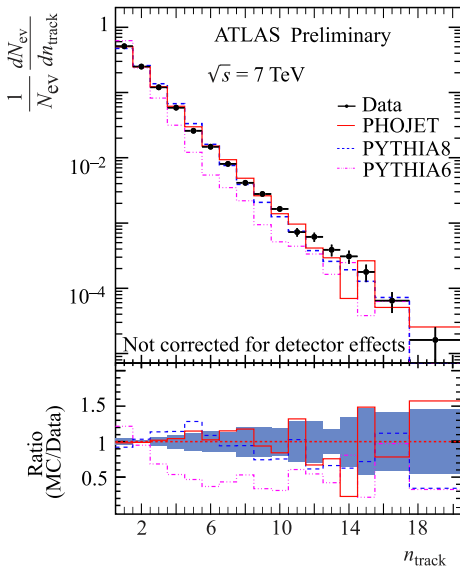


Fig. 7. The multiplicity track distributions for the single-sided MBTS requirement. The data are shown in the same way as in Fig. 2

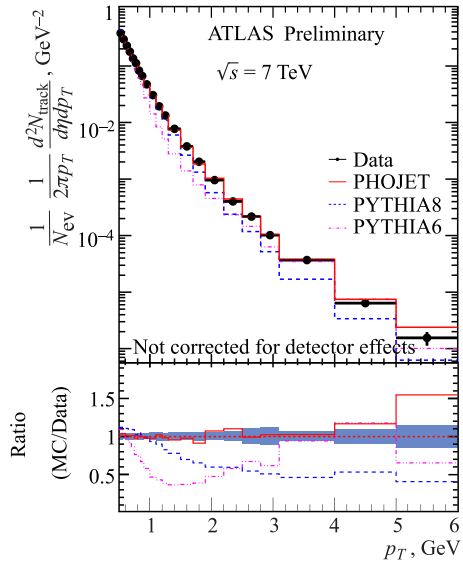


Fig. 8. The distributions of  $p_T$  for the single-sided MBTS requirement. The data are shown in the same way as in Fig. 2

In order to understand the origin of the features observed, a detailed study of the distributions for each generator was carried out with each of the subprocesses separately [5]. This confirms the importance of hard diffraction as incorporated in PYTHIA8 and indicated a need of an increase of the nondiffractive component both in PYTHIA8 and in PHOJET relative to PYTHIA6.

<sup>1</sup>Here  $\Delta\eta$  is the absolute value of the difference in pseudorapidity between the edge of the MBTS detector that has no hit ( $\eta_{\text{MBTS}}$ ) and the track, i.e.,  $\Delta\eta = |\eta_{\text{MBTS}} - \eta|$ , where  $\eta_{\text{MBTS}}$  is +2.08 or -2.08 depending on which MBTS side did not have any hits.

## CONCLUSIONS

Using the first proton–proton data obtained at the LHC, soft QCD studies are carried out by the ATLAS experiment. Charged-particle distributions are measured with the ATLAS detector at the center-of-mass energies  $\sqrt{s} = 0.9, 2.36, \text{ and } 7 \text{ TeV}$ . The measurements show good understanding of the detector and tracking performance. First measurements are performed for minimum bias events at all three energies and for diffractive events at ever large centre-of-mass energy. The results obtained are of great importance in our understanding of soft particle production processes and for improving phenomenological and Monte Carlo models.

## REFERENCES

1. Aad G. et al. (*ATLAS Collab.*) // JINST. 2008. V. 3. P. S08003.
2. Kittel W., De Wolf E.A. *Soft Multihadron Dynamics*. World Sci., 2005. 652 p.
3. *ATLAS Collab.* ATLAS-CONF-2010-046. 2010.
4. *ATLAS Collab.* ATLAS-CONF-2010-047. 2010.
5. *ATLAS Collab.* ATLAS-CONF-2010-048. 2010.
6. Bélanger-Champagne C. This workshop, P. 34.
7. Aad G. et al. (*ATLAS Collab.*) // Phys. Lett. B. 2010. V. 688. P. 21.
8. Sjostrand T., Mrenna S., Skands P. Z. // JHEP. 2006. V. 05. P. 026.
9. *ATLAS Collab.* ATL-PHYS-PUB-2010-002. 2010.
10. Marshall Z. // Conf. Note ATL-SOFT-PROC-2008-001. 2008.
11. *ATLAS Collab.* ATLAS-CONF-2010-031. 2010.
12. Skands P. Z. arXiv:0905.3418 [hep-ph]. 2009.
13. Albrow M. G. et al. arXiv:0610012 [hep-ph]. 2006.
14. Sjostrand T., Mrenna S., Skands P. Z. // Comp. Phys. Commun. 2008. V. 178. P. 852.
15. Egel R. // Z. Phys. C. 1995. V. 66. P. 203.